RESEARCH ARTICLE

Experimental validation of a wireless monitored solar still for efficient olive pomace drying and distilled water production

Antonio Rodríguez Orta[a], Roque Aguado Molina[b], Manuel Sánchez Raya[a], David Vera Candeas[b] and Juan Antonio Gómez Galán[a]

[a]Departamento de Ingeniería Electrónica, Sistemas Informáticos y Automática, Escuela Técnica Superior de Ingeniería, Universidad de Huelva, Avda. de las Fuerzas Armadas s/n, 21007 Huelva, Spain
[b]Departamento de Ingeniería Eléctrica, Escuela Politécnica Superior de Linares, Universidad de Jaén, Avda. de la Universidad s/n, 23700 Linares, Spain

ARTICLE HISTORY
Compiled May 13, 2025

ABSTRACT
This work presents the prototype of a solar still that can be used as a complement to the traditional fossil fuel-based drying process of olive pomace, a thick sludge with a high moisture content that is massively by-produced in the olive oil industry. In addition, the system allows to recover distilled water, which can be used to irrigate the adjacent fields. The feasibility of the system for the target application was experimentally validated by designing a wireless data acquisition circuit for data collection, remote storage, visualization and analysis in real-time, with access possible from multiple devices. The results from a test campaign revealed that the moisture content of the olive pomace was effectively reduced from 67.17% to 39.90% in a 10-day period. A maximum drying efficiency of 16.64% was achieved, with potential for higher values under favorable weather conditions. The simplicity of the design and the low-cost solution can facilitate the future large-scale implementation of a similar system.

KEYWORDS
Solar drying; Moisture; Waste-to-energy; Prototype; Real-time system; Monitoring

1. Introduction

In the Mediterranean areas of southwestern Europe, there is a significant concentration of agro-industrial activities that generate large amounts of waste. Particularly, olive pomace (also called *alperujo*), a by-product from the olive oil production process, is a major problem for oil mills, due to its enormous production rate, its substantial polluting potential, and the high costs associated with its management (*1*). Olive oil production is an ancient practice that has undergone innumerable changes throughout its long history, and with these improvements in production methods, the yield and physicochemical characteristics of the by-produced waste streams have also been modified. Currently, more than 90% of the oil mills in Spain use the extraction method based on two-phase decanters, which produce on the one hand virgin olive oil, and on

CONTACT J.A. G.G. Author. Email: jgalan@diesia.uhu.es

the other hand, olive pomace (2). Fig. 1 provides a graphical overview of the different inflows and outflows in the olive oil production process.

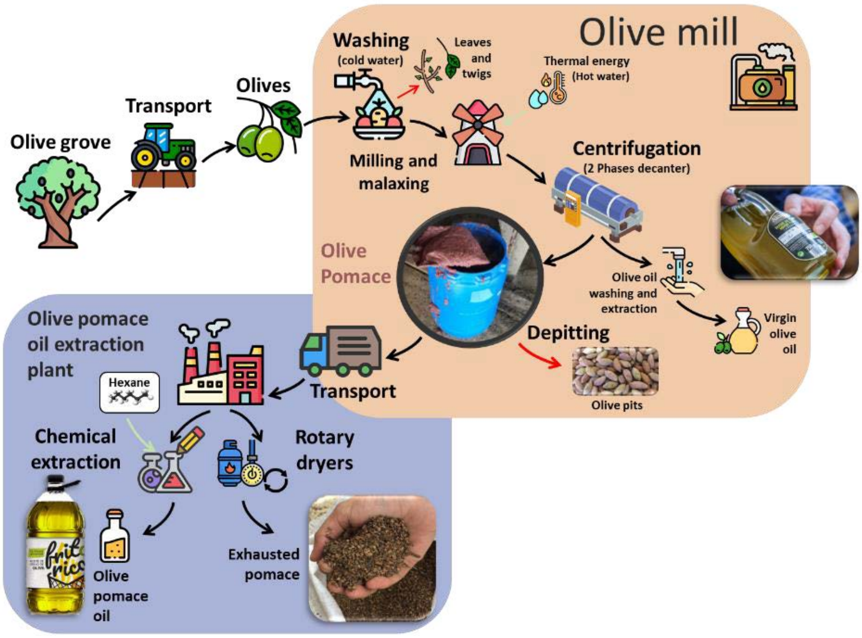

Figure 1. Products and by-products of the olive oil industry (two-phase extraction process).

Olive pomace constitutes the most important by-product of the Spanish olive oil industry in terms of production rate. It presents the appearance of a thick sludge, with a high moisture content (60–70% in wet basis) (3–5). This sludge is formed as mixture of the skin, pulp, and crushed pits of the olives, and has an olive oil content of 2–4% by weight (3). The remaining oil is known as olive pomace oil and is typically recoverable through chemical processes. However, a major issue for the management of olive pomace is its high moisture content and acidic pH (5.4) (6), which hinder the process of reusing the material, as well as the storage, transport, and drying tasks due to its high fluidity.

The most widespread practice for the management of this inconvenient waste consists of its transportation to olive pomace oil extraction plants, where, through mechanical and chemical processes, the remaining olive pomace oil is extracted. Beforehand, an energy-intensive drying process of the olive pomace is typically carried out, using large-scale continuous rotary drum dryers (4, 7, 8). Rotary drum dryers work extensively using natural gas as source of thermal energy, which is a costly solution, especially due to the increasing prices of fossil fuels. The hot flue gases from the combustion chamber discharge flow often through the dryer in a co-current flow direction (9). The dried pomace eventually undergoes a process of solid-liquid extraction of crude pomace oil with an organic solvent, usually hexane, obtaining as a result a by-product known as exhausted olive pomace (also called *orujillo*) (7). This by-product is an interesting solid biofuel, given its low moisture content of around 10–15% and its average calorific value of approximately 4200 kcal/kg (∼17.5 MJ/kg) on a dry basis (8, 10). Accordingly, this work aims at developing a low-cost solar still prototype that can be used as a complement to the drying stage, traditionally performed in continuous drum dryers, which would contribute to reducing the consumption of natural gas and the energy bill of olive pomace extraction plants, by substantially reducing the moisture content of the feedstock. Although a considerable amount of data is available in the literature on the design and performance of solar dryers for agricultural products, there are just a few studies regarding solar drying processes of wet agri-food waste for energy use (*11*). Moreover, the proposed prototype is characterized in that the extraction of the moisture contained in the olive pomace is produced through condensation of water drops on the inner surface of a glazed cover with a certain inclination, instead of water vaporization by means of forced convection. Thus, a significant fraction of the moisture contained in the wet feedstock can be recovered for irrigation purposes. The design characteristics of the developed prototype are thoroughly addressed below in section 3.1.

On the other hand, a thorough assessment on the performance of the proposed prototype for drying olive pomace involves the collection of large amounts of data. However, the efficient acquisition, management and analysis of the data can turn into a tedious, time consuming, and costly process. In most research works, these large volumes of monitored data are input manually into computer files for storage and subsequent analysis. This labor-intensive procedure is also prone to potential transcription errors, which makes important the automation of the data acquisition process, together with the storage-file creation and analysis of the data. Data acquisition circuits are widely used in renewable energy applications in order to gather data regarding the installed system performance (*12*, *13*). To this end, a low-cost, battery-operated, microcontroller-based, autonomous data acquisition circuit was developed and applied to the continuous monitoring of the olive pomace drying process. The circuit collects, stores, and transmits the data to a computer for archival storage, as well as for remote performance analysis. The design requires devices small in size to facilitate the deployment, and limited power consumption due to their battery-powered operation. In this way, hardware components were chosen to assure functionality, accuracy, and low power consumption. The compact design and the wireless approach ensure a convenient installation for placement on the dryer prototype, and easy maintenance. The energy supply is assured during the field work by a battery-charging solar panel. Moreover, a reliable and robust packaging was also designed to protect the data acquisition board. The features of the developed system for data acquisition, management and analysis are discussed in sections 3.2 and 3.3.

2. Literature review

Drying is a widespread practice in the agri-food industry, since it reduces the appearance of diseases and pests, in addition to supporting product preservation and reducing food spoilage (*14*, *15*). Hence, this practice has been studied with a multitude of tests and has been applied to different edibles. Traditionally, the drying of food was carried out by exposing the food to the sun, but in the industrial scale, drying soon became dominated by fossil fuels, which involved an increase in production and a reduction in the surface required for the drying process. Currently, due to the growing concerns on safeguarding the environment from the adverse effects of climate change triggered by greenhouse gas emissions, along with the increasing trend in the cost of fossil fuels, different alternatives have been sought to improve the performance of drying processes with the contribution of knowledge and innovative technologies. Solar dryers, also called solar distillers, are classified based on how solar radiation strikes and how the air circulates, having direct, indirect, or mixed radiation, and natural or forced convection of the air (*15*–*17*). Ekechukwu et al. (*18*–*20*) reviewed diverse types of solar dryers, using direct, indirect, or mixed radiation, demonstrating that forced convection dryers are more effective than those using natural circulation, although their cost is prohibitive for small applications.

2.1. *Direct solar dryers*

In this process, the radiation directly affects the product to dry, so that the moisture of the product is taken up by the air that surrounds it. In these cases, it is necessary to move the substance to be dried in order to distribute the humidity. Over the years, different studies and alternatives have been proposed for this type of drying. Three different types of solar dryer, based on natural and forced convection, were investigated experimentally by Sharma et al. (*21*). Their results indicate that cabinet-type solar dryers based on natural convection are well suited for drying small amounts of fruits and vegetables, making them appropriate for household scale. For large quantities, suitable for usage at scales ranging from household to industrial, or farm scale, an indirect, multi self-dryer type can be considered. The type of product being dried can also affect the performance of the dryer. A study conducted by Sehery et al. (*22*) compared the performance of the different types of dryers when drying grapes, figs, tomatoes, and onions. For a mixed mode dryer, grapes with an initial moisture of 83% are dried to a moisture content of 30%, at an average temperature of 55 °C, in 4 days, while natural drying reduces the moisture to as low as 57% in the same period, at an average temperature of 27 °C. For an indirect mode solar dryer, in a period of 8 days, the moisture content could be reduced to as little as 16.5%, while in the same drying duration natural drying reduced the moisture content to 43%. Other factors that impact the performance of the solar dryer is the combination of solar dryer type and air flow. Castillo-Téllez et al. (*23*) performed an experimental work on drying stevia leaves, reducing their moisture from an initial value of 80% to a final value of 10% in 9 to 10 hours. Their experiments were conducted using a direct-type solar dryer under natural and forced convection, as well as an indirect-type solar dryer. They concluded that the indirect-type solar dryer is more effective due to its drying time, and its controlled operation conditions. VijayaVenkataRaman et al. (*24*) reported that agricultural products such as coffee, tobacco, tea, fruits, cocoa beans, rice, nuts, and wood require drying by a constant application of low heat. It is in this category of drying at low temperature (50–60 °C), where the present work on the drying of olive pomace focuses.

2.2. *Indirect solar dryers*

In indirect solar dryers, solar radiation is captured by a collector where a certain amount of air circulates. This air, which is responsible for performing the contact drying of the product, is heated and enters the drying chamber (*25*). In turn, within the indirect dryers, depending on the way in which the collector-drying chamber system is integrated, three types may appear: the indirect ones, in which the drying chamber does not allow the entry of solar radiation; the direct ones, in which the chamber receives solar radiation; and the mixed ones, in which the radiation can be received both by a previous collector and by the drying chamber. Sharma et al. (*26*) presented the design and performance analysis of an indirect-type solar dryer designed for drying 90 kg of grapes, with an initial moisture of 80%, to a final value of 15%, in a period of 5 to 7 days. Among their observations, is an increase in the efficiency from 44% to

61% as the mass flow rate increases. Furthermore, the drying process is very fast in the first hours, with the drying efficiency decreasing in time. Another study on the design and operation of direct and indirect types of solar dryers was conducted by ben Mabrouk et al. (*27*), who focused on the drying of agricultural products. In their experiments, it is noticed that the product temperature is higher than the air inlet and outlet temperatures, of 40 °C and 27 °C, respectively. The values of annual thermal efficiency for the indirect and the direct dryer types were 60% and 40%, respectively. Fudholi et al. (*28*) presented an indirect solar dryer with improved performance used for drying 100 kg of palm oil fronds from an initial moisture content of 60% to a final value of 10%, in just 22 hours. A variety of parameters were recorded during this experiment, such as the solar radiation, ranging from 96 W/m^2 to 1042 W/m^2, the drying chamber air temperature, ranging from 26 °C to 67 °C, the inlet temperature of the drying chamber, with values from 26 °C to 75 °C, the outlet temperature, ranging from 25 °C to 65 °C, as well as the air flow rate, with a value of 0.13 kg/s. The main performance parameters of the system were a collector efficiency of 31%, 19% drying efficiency, and an efficiency in the moisture pick-up of 67%.

While the forced convection dryer appears to be superior to the natural convection type, there is a limit in the velocity of the circulating air. An experimental study on this limit was conducted by Shamekhi-Amiri et al. (*29*), in a fabricated indirect solar dryer that was used to analyze the performance of drying lemon balm leaves in a double-pass forced-convection mode. In their work, two cases were compared: a first case with values for solar irradiation of 600 W/m^2, atmospheric temperature of 22 °C, mass flow rate of 0.00615 m^3/s and collector outlet temperature of 38 °C, and a second case with values for solar irradiation of 900 W/m^2, atmospheric temperature of 25 °C, mass flow rate of 0.01734 m^3/s and collector outlet temperature of 68 °C. The results showed an increase of 20% in collector efficiency from the first to the second case. However, if the mass flow rate was further increased to 0.034378 m^3/s, an adverse effect was obtained.

2.3. *Mixed mode solar dryers*

A system that resembles the sun drying using a far-infrared heater panel was designed and tested by Nindo et al. (*30*) for drying rough rice. A particularly important aspect in the drying process was the creation of a uniform temperature within the bed, which was achieved by mixing. This also reduced the crack damage of the grain, as well as helping achieve a faster drying. For a 6 cm thick bed, the system was capable of reducing the moisture content by 0.4% per hour, which is slightly faster than the non-mixed drying of a cm thick bed. Another system, designed and constructed by Zomorodian et al. (*31*), tests both the forced-convection indirect, as well as the mixed-mode, solar drying of sultana grapes that have an initial moisture content of 78%. Various flow rates, of 0.085, 0.126 and 0.171 kg/s, were used in the experiment. One of the findings from this experiment is that there was a diminishing rate of moisture ratio decrease depending on the air flow rate. Baniasadi et al. (*32*) evaluated the performance of a mixed mode solar dryer that incorporates thermal energy storage. The system was used for the drying of an apricot and plum sample with an initial moisture content of 86%. It achieved a moisture removal efficiency of about 10%, while its thermal efficiency is around 11%. The thermal storage has the effect of reducing the drying time by 50%, with the addition of a fan. The highest temperature reached by the dryer was 65 °C, while its fastest drying rate was 2.1 g/h. Similarly, Yassen et al. (*33*) developed a solar-thermal hybrid drying system for drying red chilies and managed to improve the drying efficiency by 3%, thanks to the incorporation of a recovery dryer. Another alternative configuration was presented by Perea-Moreno et al. (*34*), who designed a greenhouse structure for drying wood chips, with the aim of creating biofuel, which was able to reduce the moisture content of the sample from 50 to 20% in just 15 days.

3. Methodology

The methodological approach for this work is divided into three parts. First, the mechanical design of the solar still prototype is addressed, along with the description of its operating characteristics for drying the wet olive pomace sample and recovering the condensed moisture. Next, the hardware design is described, including the instrumentation, sensors and data acquisition circuit. Finally, the main features of the firmware are presented.

3.1. *Solar still, mechanical design*

The proposed solar still is a modified solar dryer by the action of the greenhouse effect (indirect solar dryer), which includes a system to favor the condensation and extraction of the moisture contained in the olive pomace. In order to evaluate this design, a prototype of reduced dimensions was manufactured, which allows to obtain an acceptable amount of water, but at the same time is easily transportable. Since the prototype solar still has no moving parts, its operation on a small scale can be perfectly extrapolated to a large dryer. This design allows the maintenance and evaluation of the prototype, without the need to use specific machinery to move the assembly. Fig. 2 shows the structure of the solar still prototype, with dimensions 590 × 690 × 700 mm (height, width, depth). The prototype is made of grade 304 stainless steel, an austenitic chromium-nickel stainless steel that is non-temperable, non-magnetic, type 18-8. Moreover, in order to reduce heat losses to the outside environment and promote the greenhouse effect, the internal walls of the prototype are thermally insulated with polystyrene.

The main objective of the proposed system is to reduce the moisture content of the olive pomace samples deposited inside. For this purpose, it is necessary to favor the increase in the internal temperature with respect to the external temperature through the greenhouse effect. The system must be placed outside and must withstand the harsh environmental conditions of the province of Jaén (Spain) during the olive harvesting campaign and oil production season (from October to February), as well as being resistant to corrosion, since olive pomace has an acidic character. Additionally, the system must be able to be moved when loaded, so it must be robust enough to withstand the forces it may suffer during transport, without disassembling. All these factors along with others, such as the cost of the prototype, were taken into consideration in the choice of materials, prioritizing the use of standard elements such as hinges, which allow the opening of the upper cover to load the samples.

In order to illustrate the construction of the solar still prototype, a schematic 3D view and exploded-view drawing is presented in Fig. 3. For construction of the structure, grade 304 stainless steel was used because, in addition to providing solidity to the structure, it is resistant to corrosion. But as steel is a particularly good conductor of temperature, which could be a problem on winter days, by favoring the discharge of heat into the environment, the system was insulated by incorporating polystyrene in

Figure 2. Photographic image of the solar still prototype.

an arrangement commonly known as "sandwich panel" (steel-polystyrene-steel), with a thickness of about 50 mm.

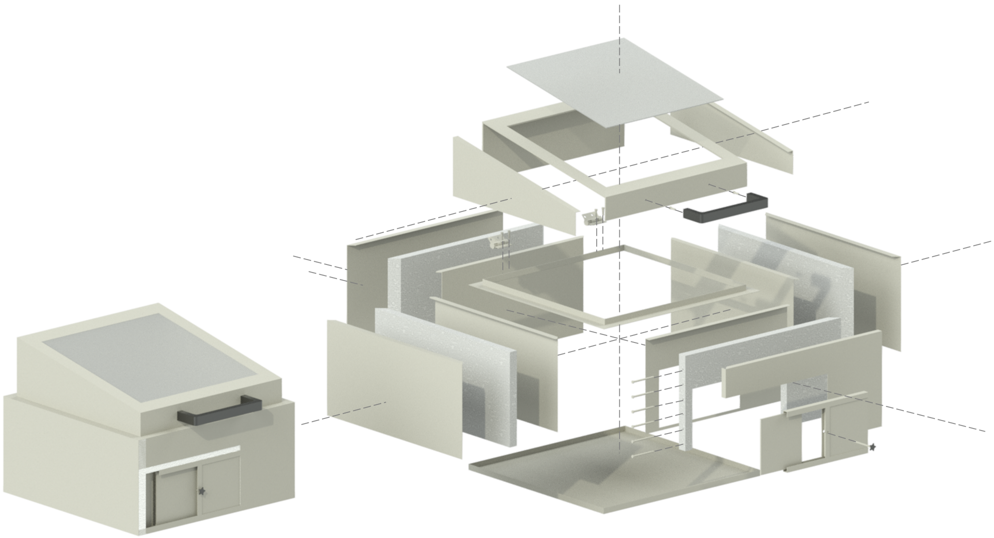

Figure 3. 3D view and exploded-view drawing of the solar still prototype.

Moreover, the system has a sliding door at the front that allows inspection of the sample during the drying process, as well as removing all the excess material that crosses the perforated platform, similarly to a sieve, on which the sample material is placed. This excess material is mostly residual oil, but also minor amounts of olive pomace that can slide through the holes. However, it represents an improvement over placing a completely sealed platform, since oil stratification hampers the drying process.

The cover of the system has a glazed window of 600 × 600 mm, which in addition to enhancing the greenhouse effect, works as a cold point that, when in contact with the vapor released due to the increase in the inside temperature, facilitates condensation. This window was made of glass with low iron content, since this material has low coefficients for absorption and reflection of radiation, which favors that the long-length solar waves remain enclosed inside the container (greenhouse effect). Thus, the use of low-iron glass improves the emission inside the system, but without leading to an increase in the temperature of the glazed surface, due to its low absorption coefficient. Thereby, the temperature gradient with the outside environment is guaranteed, considering the relatively low ambient temperatures that surround the system during the olive oil production season.

To favor the evacuation of condensed moisture to the outside, the glazed window was placed with an angle of inclination of 30° with respect to the ground. The water drops slide down the inclined glass by the action of gravity toward an inner gutter positioned flush with the glass. Finally, the collected water is stored in an external tank, which is filled by a hose that connects the prototype with the storage system, which has an angle of inclination with respect to the ground of about 15° to facilitate discharge of the condensed moisture. The final prototype was placed on the terrace of the EPS Linares laboratories (DMS coordinates: 38°05'04"N 3°38'46"W), facing south.

3.2. *Hardware design*

In order to evaluate the performance of the system and be able to monitor the evolution of the environmental conditions inside and outside of the solar still prototype, a customized data acquisition circuit was developed. Thus, the prototype was instrumented with sensors connected to an electronic board designed with components that occupy the least possible space, and with wireless connectivity to send the data remotely, avoiding having to open the system once the drying process is ongoing, which would modify the results obtained due to the loss of heat and vaporized moisture. The most relevant parameters to be monitored are the temperature and humidity of the air, which are measured in the upper and lower areas inside the dryer, along with the environmental values, as indicated in Fig. 4. The placement of the humidity and temperature sensors inside the prototype aims to help understand how the drying process occurs, as well as to verify whether the selection of the insulation material was correct. Nevertheless, the wireless electronic board is flexible and can be scaled up by adding more sensors to improve accuracy, or more sensor types to measure other physical magnitudes or parameters of interest. In addition, a standardized solar irradiation meter was placed in the vicinity of the prototype, to evaluate the performance of the system considering the amount of water extracted and the solar radiation captured.

The diagram of the data acquisition circuit is shown in Fig. 5. The system basically consists of a control unit that collects all the measurement parameters, a real-time clock (RTC), and the power supply system. The sensors used in the design are readily available low-cost devices, which provide enough accuracy to extract the relevant data from the experiment. Data samples include timestamps to determine the corresponding elapsed time of the experiment. Considering the wireless nature of the data collection, it is essential to ensure that there is no loss of data, resulting from wireless communication between the computer and the data acquisition board.

The processor of the control unit is an ESP32 from Espressif Systems. This SoC (System on Chip) integrates a 32-bit Tensilica Xtensa LX6 main microprocessor and an ultra-low power coprocessor, peripheral interfaces for communication with several

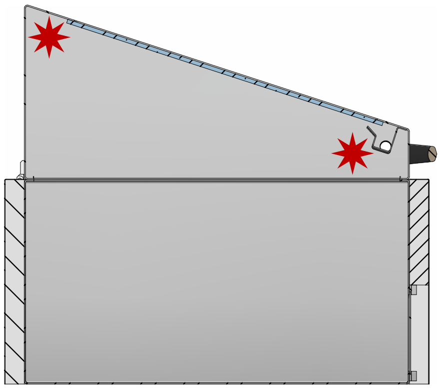

Figure 4. Cross-section view of the solar still prototype with the sensor placement locations (red stars).

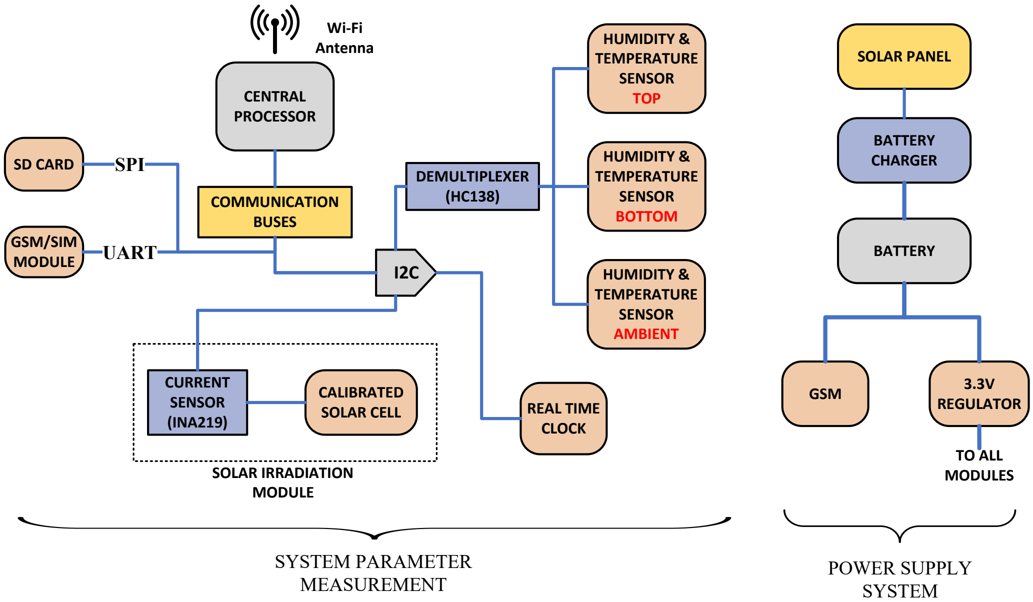

Figure 5. Block diagram of the data acquisition circuit.

types of external elements, and wireless connectivity including Bluetooth and a Wi-Fi transceiver that provides remote data communication. The design is completed with the following additional elements:

(a) *Real-time clock*: Based on the DS3231, it maintains temporal synchronization of the processor to provide a timestamp to each measurement block taken by the system.

(b) *Memory card*: it is used for the local data storage of both measurement data and diagnostic messages. Thus, it provides a backup system in case of network loss, sending data once the connection is restored. This memory can be extracted and connected to a computer to access its stored information. Data communication is made through SPI.

(c) *Solar irradiation measurement module*: The value of solar irradiation is obtained by measuring the output current of a previously calibrated solar cell (Atersa, Grupo Elecnor, Spain). The solar cell is rated IP65 in the ingress protection code (IEC 60529), and hence, it can be safely placed outdoors. The measurement results are provided using the 4–20 mA standard, which corresponds to measurements from 0 to 1200 W/m^2. The electric current is measured by means of a module based on the INA219 sensor, which performs the conversion from analog to digital, and sends the collected value to the central processor through I2C communication.

(d) *Power supply system*: it consists of a solar panel, a standard Lithium battery type 18650 and a battery charging circuit. This module enables a battery-powered operation of all the elements of the system, without requiring electricity grid connection. Due to the low power consumption of the system and the fact that the sampling interval is 10 minutes (139 samples per day), the system can be in continuous operation for 31 days without power supply. However, under typical operating conditions, the battery will always be charged during the daylight hours thanks to the 6 W photovoltaic panel.

(e) *Temperature and humidity measurement*: this is provided by two SHT20 devices, which have a resolution of 0.04% RH and 0.01 °C, for relative humidity and temperature, respectively. These I2C sensors have the same predefined access address and are not programmable. Thus, in order to communicate with several devices, an HC138 digital demultiplexer of 3 to 8 lines was used. The sensors are connected to the system through four wires, two for power connection and two for data transmission. Shielded cables were used to prevent electrical noise. Each sensor is placed in a waterproof plastic case to offer mechanical protection and protection from condensation. The cases are provided with openings made of porous materials to allow the temperature and humidity measurement. In addition, the sensor's PCB and cable connections to the sensor board were covered with a protective layer of acrylic sealant to prevent corrosion.

(f) *SIM module*: this element is in charge of establishing the communication with the mobile network by means of a GSM/GPRS protocol, which sends the data to the remote storage server for further consultation. This module provides more flexibility to the installation, as it is not limited by the Wi-Fi connectivity.

3.3. *Firmware*

The system implements a version of FreeRTOS adapted by the manufacturer of the microcontroller. This RTOS (real-time operating system) is responsible for managing the different buses, such as, UART, SPI, I2C, etc. as well as the functions necessary for the transfer of information through the TCP/IP protocol. This method allows tasks to be parallelized, based on priorities defined by the programmer. This alternative of task control saves resources, leaving the handler to assign tasks, based on the priorities defined above. To illustrate the operation of the system, Fig. 6 shows the sequential flowchart. However, the processes run in parallel except for the start-up and the switching to low-power mode.

The data acquisition circuit has four main tasks: Wi-Fi connection, firmware update, sensor capture, and data sending. When the system boots, all tasks start at the same time, but the task of sending data to the server and the task of updating firmware wait for a successful connection to the Wi-Fi network. At the same time, the sensor capture task makes a capture cycle and stores the readings on the SD card. If an Internet connection has not been achieved within a reasonable time, the system goes into sleep mode until the time between sampling (10 minutes) has passed. If an Internet connection is achieved within a reasonable time, the system checks the SD card for

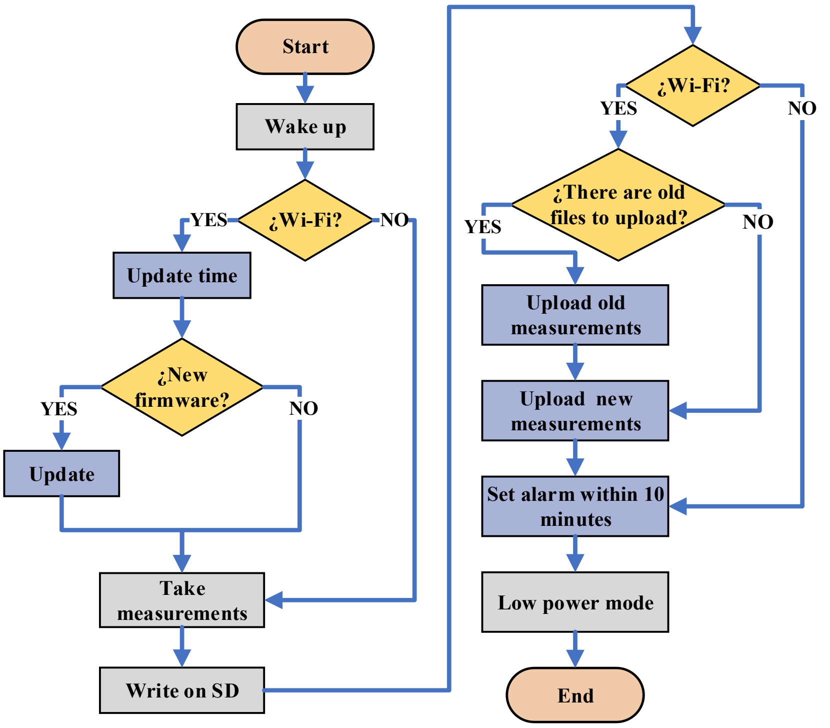

Figure 6. Summary flow chart of the firmware.

outdated data (both internal system data and measurement data) and, if any, it is sent by marking them as sent.

Among the checks carried out when a connection with the Wi-Fi network is established, is the one made by the firmware update task. It connects to the local server and verifies if the firmware needs to be updated. In case of an update, the system receives the data and stores it in an alternative flash partition, waiting for the pending tasks to be completed in order to restart the system. To perform this OTA (Over The Air) update, the program memory is divided into two parts, alternating between them for every change of version. Finally, to ensure that the system has the time correctly indexed, there is a special task that updates the time and date of the PSTN through the internet connection, making use of the NTP protocol. This task is performed a long time after the last RTC update. The system was programmed to send data to two different servers:

Local server: Sends the data along with the diagnostic information to a local server where it is stored and can be queried locally or remotely. In addition, this local server allows the user to evaluate the operation of the system, as well as to have diagnostic data available locally in case any problems arise.

Ubidots: the data is uploaded to the Ubidots platform in JSON format, which allows for its analysis in real time in the IoT (Internet of Things) portal.

4. Results

The solar dryer prototype was operating outdoors for several months in 2021 in order to verify that the assembly could withstand the passage of time, exposed to inclement weather without any intervention of the users, making the data acquisition circuit a continuous monitoring of the differences in temperature and humidity between the interior and exterior of the assembly. These test conditions were maintained until the month of October, which is when the olive harvest period begins.

The test campaign of the prototype was carried out during the period 9–18 of October 2021, monitoring the evolution of the environmental characteristics, as well as the moisture contained in an olive pomace sample. For this purpose, a sample of 11.28 kg of olive pomace was used. The olive pomace was supplied by the olive oil mill "SCA Santo Tomás" (Santo Tomé, Jaén, Spain). The moisture contained in the sample was measured to know the initial state of the product. During the drying process, samples were taken every 2 days and sent to the laboratory and to determine the evolution of their heat of combustion and moisture content.

4.1. *Calculation of the moisture content*

The olive pomace was characterized through a series of chemical analyses, which were performed in triplicate after weighing of the samples to ensure reproducibility. The amount of water extracted can be determined at the end of the drying process by simply observing the difference in mass. An analytical procedure based on UNE-EN ISO 18134-1:2016 standard was followed when conducting the drying process, but making sure that the dryer temperature does not exceed 85–90 °C, since at higher temperatures other volatile compounds tend to evaporate, introducing errors in the results. In order to completely dry the samples, they must remain in the oven until after two consecutive measurements, taken at intervals of 12 hours, their weights remain virtually unchanged (weight difference below 1%). The laboratory results of the weighing are shown in Table 1, with an average moisture content of the samples equal to 67.17%. It is noteworthy that the amount of moisture present in the sample can be expressed on a wet basis (W) or on a dry basis (Y), as given below (*32*, *35*).

$$W = \frac{m_i - m_f}{m_i}, \quad \text{wet basis (wb)} \tag{1}$$

$$X = \frac{m_i - m_f}{m_f}, \quad \text{dry basis (db)} \tag{2}$$

where:

- W = Moisture content in the sample, wet basis (kg moisture/kg wet sample).
- X = Moisture content in the sample, dry basis (kg moisture/kg dry sample).
- m_i = Initial mass of the wet sample loaded inside the solar still prototype (kg).
- m_f = Final mass of the wet sample loaded inside the solar still prototype (kg).

Table 1. Initial data of the olive pomace samples: Moisture content.

Sample №	Weight of the olive pomace (g)		W (wt.%), $\frac{\text{kg moisture}}{\text{kg wet sample}} \times 100$	X, $\frac{\text{kg moisture}}{\text{kg dry sample}}$
	Before drying	After drying		
Sample one	20.978	6.768	67.74	2.10
Sample two	30.551	10.029	67.17	2.05
Sample three	38.190	12.751	66.61	2.00

4.2. *Calculation of the heat of combustion*

A very common application of the olive pomace is as renewable fuel in bioenergy plants. In this regard, a reduction in the moisture content of this by-product is typically required in order to release a higher amount of heat when combusted. Therefore, a study on the reduction of its moisture content and increase of its heat of combustion during the drying process inside the solar still prototype was carried out. For this purpose, the prototype was loaded with a given amount of wet biomass feedstock and samples were extracted every 2 days.

The elemental composition of olive pomace was determined through ultimate analysis, which provides the information concerning the mass fractions of elements such as carbon, hydrogen, nitrogen, sulfur, and oxygen. A CHNS elemental analyzer (Thermo Finnigan Flash EA1112, Waltham, MA, USA) was used to determine the content of contents of carbon, hydrogen, nitrogen and sulfur in the samples, while the content of oxygen was calculated by difference. The results from these measurements, expressed in weight percentages on a dry basis, are reported in Table 2.

Table 2. Ultimate analysis of the olive pomace sample (wt.%, dry basis).

Sample №	C	H	N	S	O[a]
Sample one	44.0050	6.4260	1.2036	0.1251	48.2404
Sample two	43.9213	6.4352	1.2559	0.0784	48.3092
Average	43.9631	6.4306	1.2298	0.1017	48.2748

[a] Oxygen content was determined by difference.

For experimental determination of the heat of combustion of olive pomace, an automatic isoperibol calorimeter (series 6400, Moline, IL, USA) was used. This equipment allows calculating the Higher Heating Value (HHV) by burning a known quantity of fuel sample and measuring the amount of heat produced in the process, which is calculated from the increase in thermal energy of a liquid of known properties (such as water). For experimental determination of the HHV, the measurement must be performed with a dried sample. The HHV is then expressed at the standard temperature of 25 °C.

For most applications of solid fuels, the Lower Heating Value (LHV) is used, as the heat contained in combustion products is typically not returned to precombustion temperature. The LHV was estimated from the experimentally determined HHV, the ultimate analysis and the moisture content through Eq. (3).

$$\mathrm{LHV} = \mathrm{HHV} - \Delta h_{vap}\left(\frac{9\,\mathrm{H}}{100} + \frac{W}{100}\right) \tag{3}$$

where:

- LHV = Lower Heating Value of the sample.
- HHV = Higher Heating Value of the sample.
- H = Hydrogen content in the sample (wt.%).
- W = Moisture content in the sample (wt.%, wet basis).
- Δh_{vap} = Enthalpy of vaporization of water at 25 °C, equal to 2.4417 MJ·kg^{-1}.

An important parameter to consider when calculating the LHV of the fuel is the moisture content of the sample. Depending on the moisture content of the sample, their elemental composition will change. Therefore, the values indicated in Table 2 for the dried sample must be corrected to consider the moisture content of the wet sample whose elemental composition is to be determined. The lower heating value at constant pressure was corrected for moisture content (LHV as received, in wet basis) by using Eq. (4).

$$\mathrm{LHV_{wb}}\,(\mathrm{MJ/kg}) = \mathrm{LHV_{db}}\,(\mathrm{MJ/kg}) \times \frac{100 - W}{100} - \Delta h_{vap} \times \frac{W}{100} \tag{4}$$

The HHV of a dried olive pomace sample was measured in triplicate with the automatic isoperibol calorimeter, resulting in an average value of 4616.61 kcal/kg (∼19.32 MJ/kg). Subsequently, the LHV of the olive pomace on a wet basis was calculated according to Eqs. (3) and (4).

Table 3 shows a summary of the values obtained from the ultimate analysis of the samples, along with the moisture content and the LHV, which were measured at intervals of 2 days. As a result of the previous analyses, the wet olive pomace initially deposited inside the solar still prototype contained 67.17% of moisture (wet basis), with an LHV of 1053.44 kcal/kg (∼4.41 MJ/kg). After a 10-day period, the moisture content of the wet olive pomace sample decreased to 39.90% (wet basis), which corresponds to an LHV of 2374.01 kcal/kg (∼9.93 MJ/kg).

Table 3. Results of the ultimate analysis together with the LHV and moisture values of the sample during the experiment.

Sample №	Ultimate analysis (wt.%, wet basis)					W (wt.%)	LHV (kcal/kg)	LHV (MJ/kg)
	C	H	N	O	S			
Initial sample	14.5078	2.1221	0.4058	15.9307	0.0336	67.17	1053.44	4.41
Sample day 2	17.3494	2.5377	0.4853	19.0510	0.0402	60.53	1374.99	5.75
Sample day 4	20.5812	3.0105	0.5757	22.5997	0.0476	53.19	1730.43	7.24
Sample day 6	24.6663	3.6080	0.6900	27.0854	0.0571	43.89	2180.79	9.12
Sample day 8	25.7989	3.7737	0.7217	28.3291	0.0597	41.31	2305.73	9.65
Sample day 10	26.4214	3.8647	0.7391	29.0127	0.0612	39.90	2374.01	9.93

4.3. *Operation of the data acquisition circuit: Hardware and software*

The monitoring system was implemented by means of an electronic board assembled and designed specifically for this work. It has the elements discussed in section 3.2. Since drying is a relatively long-term process, a proper system evaluation requires for data to be measured and stored during all the drying process, to evaluate the system performance and to model the variables that affect the process. The system operates cyclically, with the main operations being data acquisition, storage, and remote communication. It wakes up periodically to take measurements for a few seconds, then returns to a state of low power consumption. As a result, a reduced average of energy is used. During clear weather days, the battery can be fully charged in as little as half an hour, from half charge to full charge. The ability to charge the battery in a reduced period is also due to the oversizing of the solar panel, ensuring battery charge even during overcast weather days. Fig. 7 shows the hardware implementation of the data acquisition circuit.

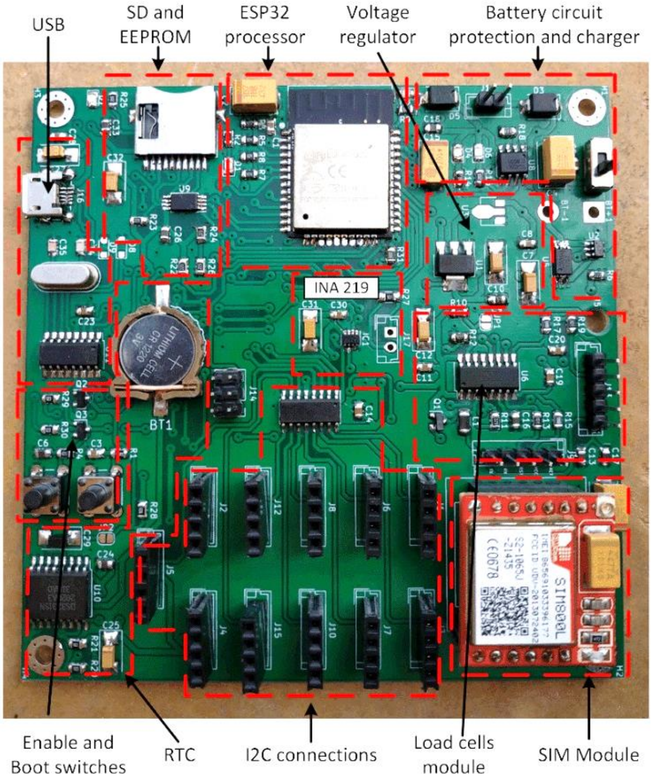

Figure 7. Hardware board of the data acquisition circuit.

The software was designed to be fail-safe, using the FreeRTOS operating system that allows the user to define a series of tasks with priority. This priority is set by the programmer, ensuring that all tasks are performed within a certain time. With this implementation of the software, the system is protected against eventualities such as a failure of the Wi-Fi network. Thus, if the system recognizes that the Wi-Fi network is not accessible, it takes the necessary measurements and goes to sleep mode, waiting until the next measurement to be taken. If when the system wakes up to take the next measurement, the network becomes accessible again, it sends all the data not previously uploaded to the server. Otherwise, it waits until the network becomes available again, repeating the power cycle, taking measurements and storing them, and then putting the system in sleep mode. In addition, if the local server is offline or the transmission of data to the Ubidots server causes a failure, the system will close the connection and go into sleep mode; then it will retry the process during the next connection cycle. Fig. 8 illustrates the graphs that the user can visualize during the operating stage of the system, implemented in Ubidots and accessible remotely.

The frequency of measurements is a remotely programmable parameter, as well as how often the data is sent to the remote server. The measured values of temperature, humidity, and solar radiation are complemented by the battery voltage and solar panel voltage values, as well as an associated timestamp that allows a date-based data classification. The data, which is uploaded to the Ubidots platform, can be viewed directly, or downloaded for further analysis, as shown in Figs. 9, 10 and 11, during the aforementioned period of study (October 9–18, 2021).

In order to verify that these measurements correspond to reality, they were compared with the data provided by different meteorological agencies, such as National

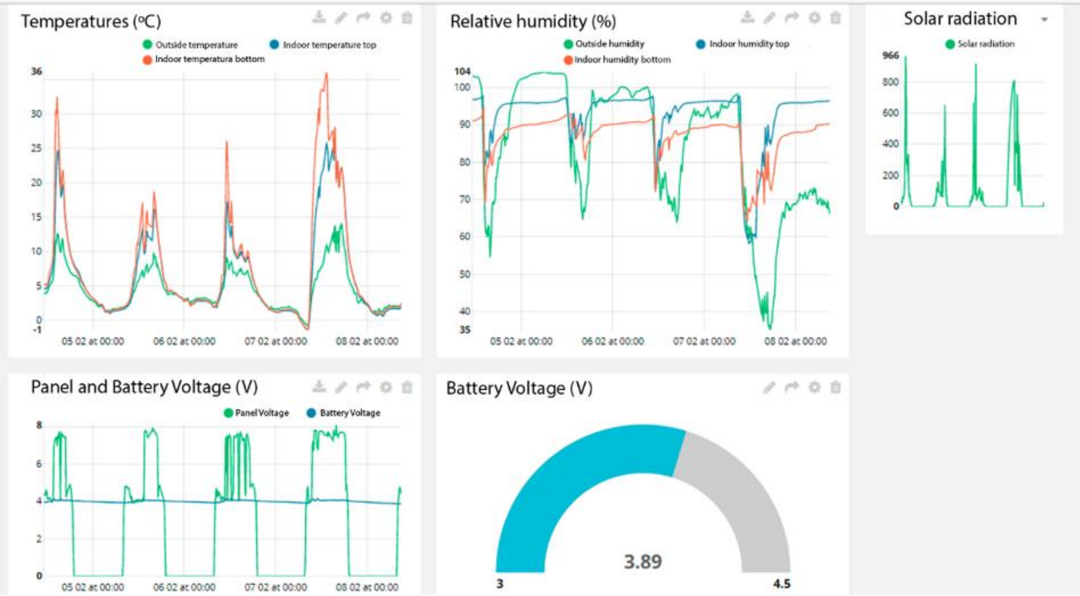

Figure 8. Control interface with graphical representation of monitored variables.

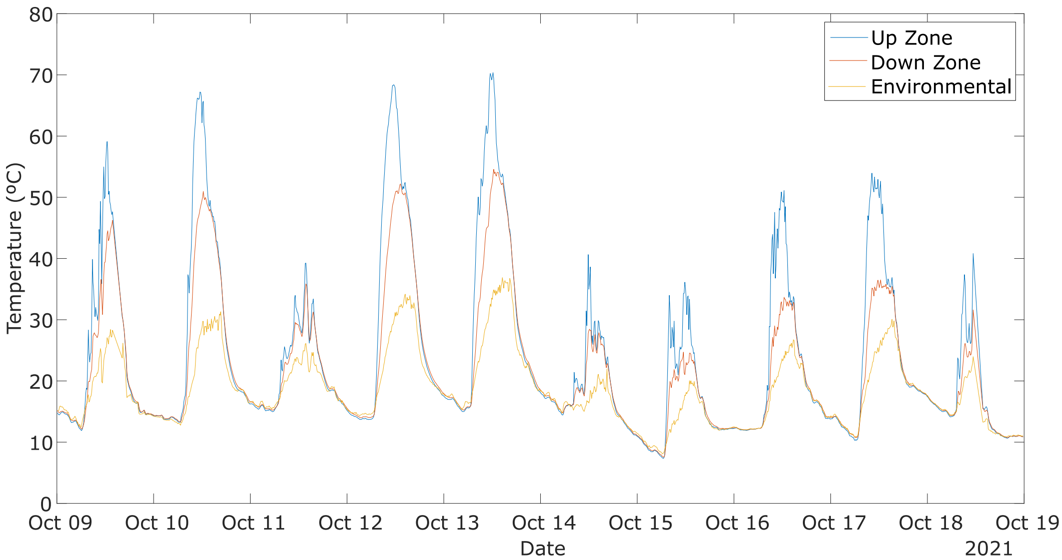

Figure 9. Temperature monitoring during the period of study.

Aeronautics and Space Administration (NASA). The POWER data access viewer tool within the Renewable Energy user community (*36*), was used to retrieve data from the nearest station, located in Andújar (Jaén, Spain), which is about 40 km west of Linares. After an exhaustive search, it was not possible to access current information from a registered weather station belonging to a recognized institution and with accessible weather measurements for the city of Linares. Despite this, the data obtained were considered as a statistical average of the last years data provided by the Andalusian Energy Agency (Spanish: *Agencia Andaluza de la Energía*, AAE) (*37*).

In accordance with the foregoing, it is noteworthy that the data for the temperature and the relative humidity are not the exactly same, but they must follow a similar

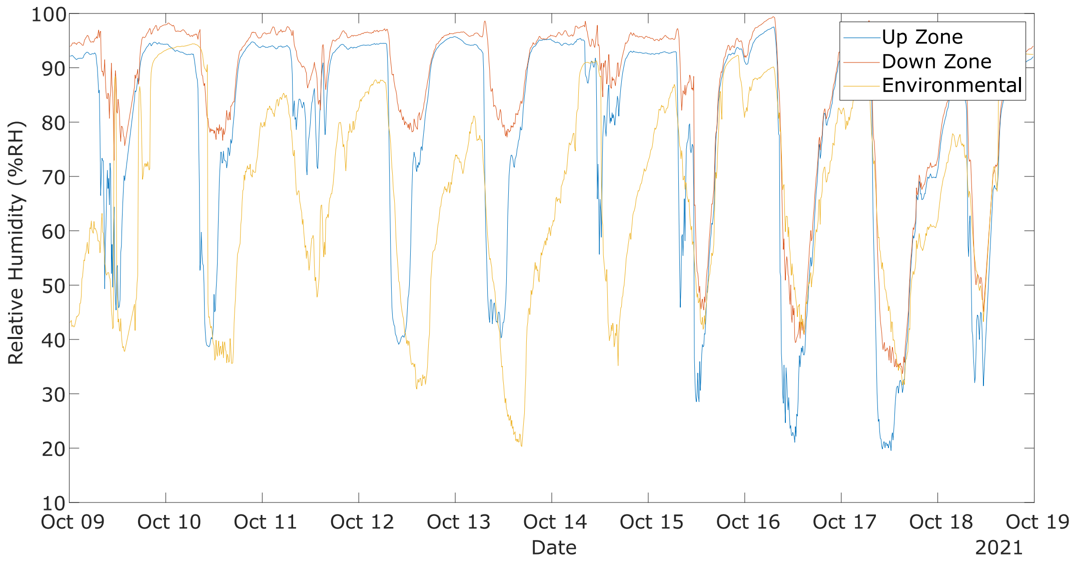

Figure 10. Humidity monitoring during the period of study.

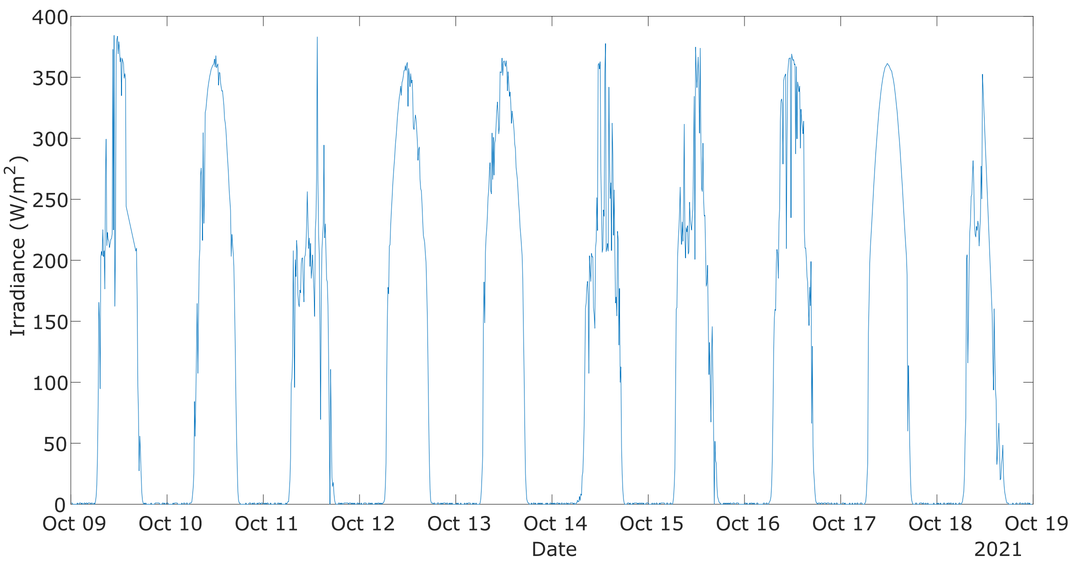

Figure 11. Irradiance monitoring during the period of study.

pattern and be within the same order of magnitude. However, what does have to be remarkably similar is the irradiation, since it presents small variation within the same province and geographical area. Nevertheless, this still allows for some peaks in the measurements to occur, as can be noted in Fig. 12, which are mostly attributed to the shading effects of clouds during the sampling period.

4.4. *Evolution of the moisture content and the LHV*

This section presents the monitoring results obtained during the 10-day period of the drying process of the olive pomace. Fig. 15 graphically illustrates the evolution

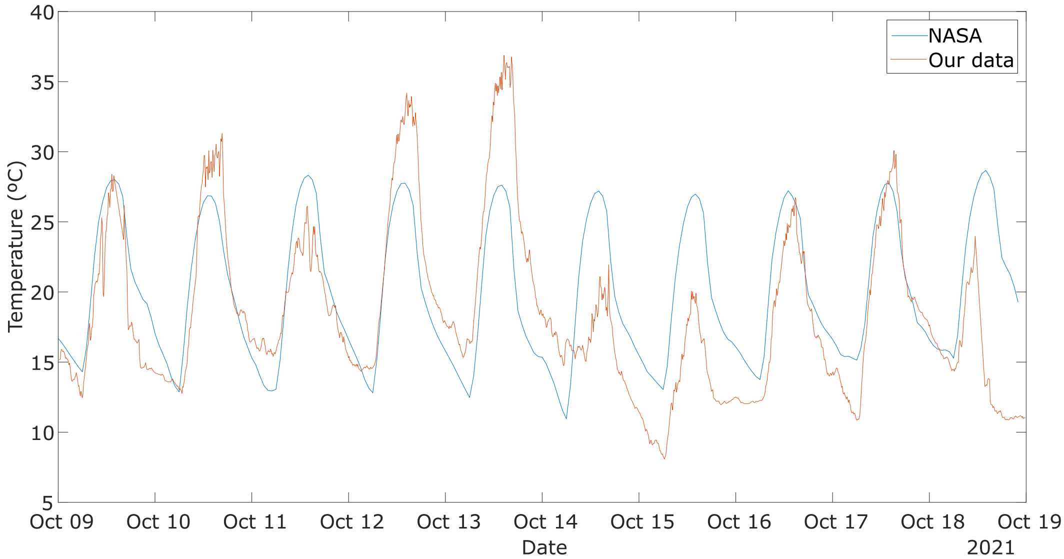

Figure 12. Comparison of the temperature registered with the prototype and the values estimated by Renewable Energy (NASA) (*36*).

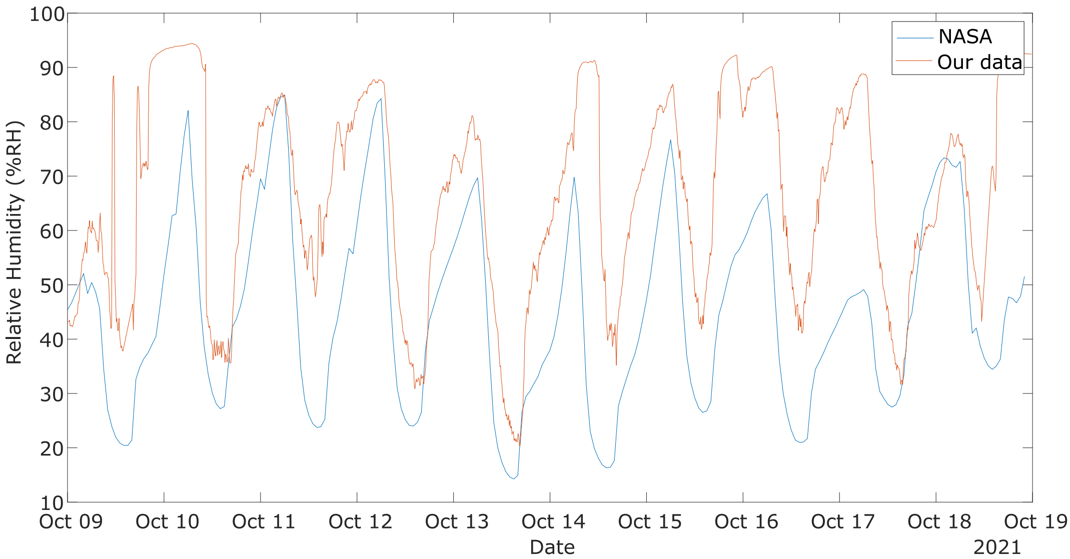

Figure 13. Comparison of the relative humidity registered with the prototype and the values estimated by Renewable Energy (NASA) (*36*).

of the moisture and LHV of the sample inside the solar still prototype, which was tested on an experimental campaign spanning the days 9 to 18 of October 2021, with measurements performed every 2 days. The moisture content of the olive pomace contained in the solar still prototype decreased from 67.17% to 39.90%, while its LHV increased substantially from 1053.44 kcal/kg (∼4.41 MJ/kg) to 2374.01 kcal/kg (∼9.93 MJ/kg) as a result of the drying process.

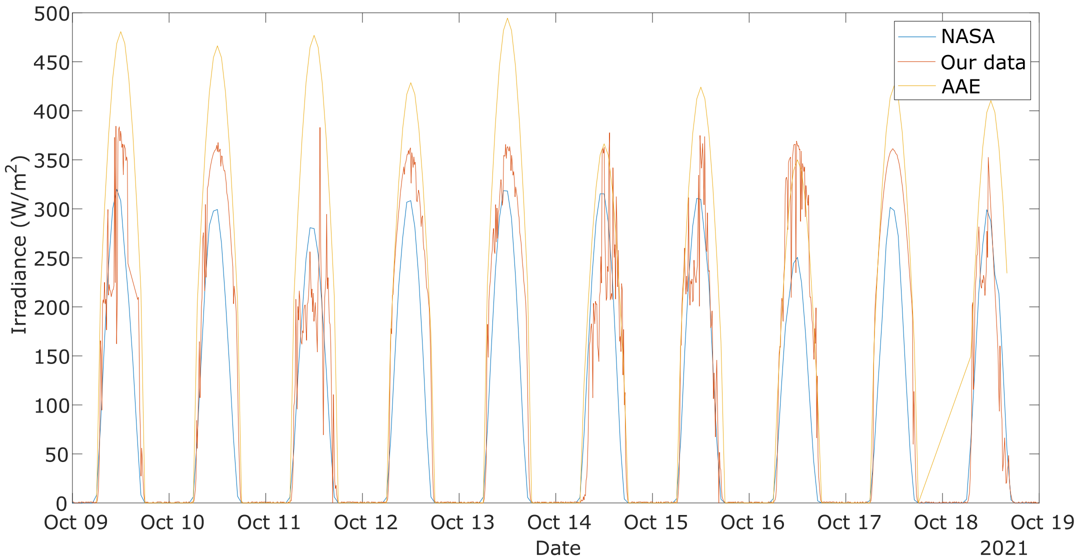

Figure 14. Comparison of the irradiance registered with the prototype and the values estimated by Renewable Energy (NASA) (36) and the AAE (mean) (37).

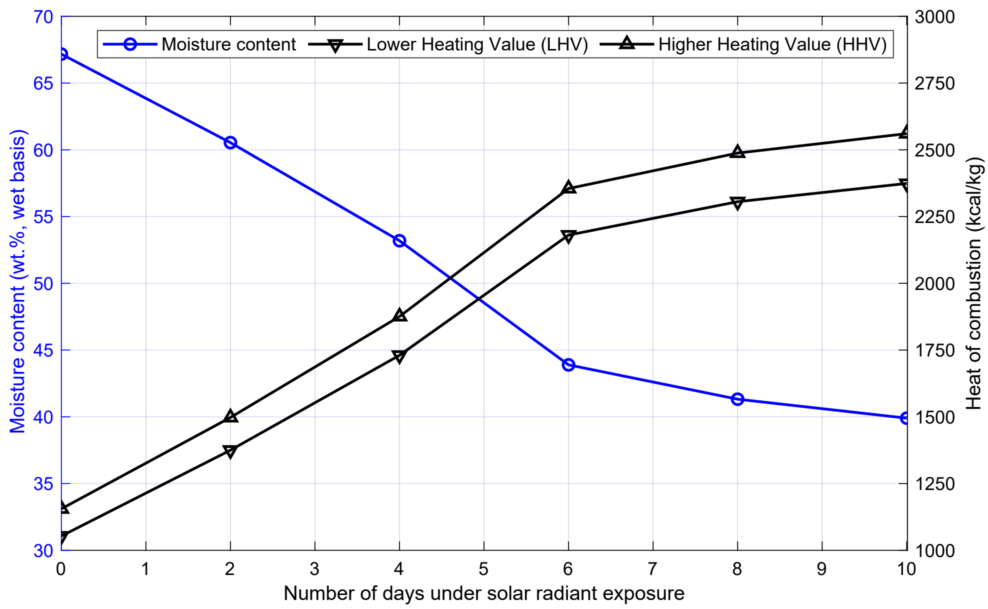

Figure 15. Evolution of the moisture content and heat of combustion with respect to the number of days under solar radiant exposure.

4.5. *Drying performance*

Another key factor to evaluate the correct functioning of the solar still prototype is the calculation of the drying thermal efficiency (η_{th}) using Eq. (5), similarly to the procedure reported by Baniasadi et al. (32). In drying processes, the drying thermal efficiency is usually defined as the ratio of the energy used for the moisture evaporation to the total thermal energy input for drying (7, 38). For the particular case of the solar still prototype, this parameter is calculated as the energy required to remove a certain amount of moisture from the sample divided by the actual solar radiant energy that reaches the glazed window (*35*). The drying thermal efficiency is also referred to in the scientific literature as system efficiency or drying efficiency (*35*). For calculation of the drying thermal efficiency, it is essential to determine the total solar radiation that fell onto the glass surface during the period of study, based on the data obtained during the monitoring shown in Fig. 11.

$$\eta_{th} = \frac{(m_i\, W_i - m_f\, W_f)\, \Delta h_{vap}}{H\, S_{glass}} = \frac{m_{dry}\, (X_i - X_f)\, \Delta h_{vap}}{H\, S_{glass}} \tag{5}$$

where m_{dry} is the mass of dry (moisture-free) sample (kg), H is the solar radiant exposure ($MJ{\cdot}m^{-2}$) and S_{glass} is the glass surface on which the solar radiation strikes (0.364 m^2). The solar radiant exposure (H) is the solar irradiance of a surface (E) integrated over the time of irradiation (t), as shown in Eq. (6).

$$H = \int_{t_i}^{t_f} E(t)\, \mathrm{d}t \tag{6}$$

Table 4 shows the evolution of the moisture content of the sample, together with the solar irradiation received by the prototype, for a 10-day period from October 9 to October 18, 2021. Measurements of the moisture content were made every 2 days and the irradiation values shown are the sum of two consecutive days. As a result, the drying efficiency was calculated by using Eq. (5) and expressed in percentage. It noteworthy that the measurements taken with the wireless monitoring system were made every 10 minutes, so the necessary calculations were done to convert from $W{\cdot}m^{-2}$ every ten minutes to $MJ{\cdot}m^{-2}{\cdot}day^{-1}$, using the trapezoidal integration rule within the intervals of hours and then days.

The time-averaged drying rate (r) is calculated according to Eq. (7) as the moisture evaporated after each two consecutive days.

$$r = \frac{m_i\, W_i - m_f\, W_f}{t_f - t_i} = \frac{m_{dry}\, (X_i - X_f)}{t_f - t_i} \tag{7}$$

Another indicator on the performance of the prototype is the specific energy consumption (SEC), which is defined as the amount of energy required by the solar still prototype to evaporate a unit mass of moisture content from the sample (*5*, *35*).

$$\mathrm{SEC} = \frac{H\, S_{glass}}{m_i\, W_i - m_f\, W_f} = \frac{H\, S_{glass}}{m_{dry}\, (X_i - X_f)} \tag{8}$$

The reciprocal of specific energy consumption is the specific moisture extraction rate (SMER), which indicates the amount of moisture evaporated per unit energy supplied to the solar still prototype (*5*, *35*).

$$\mathrm{SMER} = \mathrm{SEC}^{-1} = \frac{m_i\, W_i - m_f\, W_f}{H\, S_{glass}} = \frac{m_{dry}\, (X_i - X_f)}{H\, S_{glass}} \tag{9}$$

Table 4. Main performance parameters of the solar still prototype during the test campaign.

Day №	W (wt.%), $\frac{\text{kg moisture}}{\text{kg wet sample}} \times 100$	X, $\frac{\text{kg moisture}}{\text{kg dry sample}}$	r, $\frac{\text{kg moisture}}{\text{day}}$	H, MJ/m^2	SEC, $\frac{\text{MJ}}{\text{kg moisture}}$	SMER, $\frac{\text{g moisture}}{\text{MJ}}$	η_{th} (%)
0	67.17	2.05	-	-	-	-	-
2	60.53	1.53	0.37	31.75	15.45	64.81	14.54
4	53.19	1.14	0.41	39.30	17.28	57.88	12.99
6	43.89	0.78	0.52	38.88	13.49	74.13	16.64
8	41.31	0.70	0.15	31.50	39.41	25.37	5.69
10	39.90	0.66	0.08	28.65	65.57	15.25	3.42

The average drying efficiency after 10 days of solar radiant exposure was around 10.66%. It can be noted that there comes a time when the system reaches a peak of drying efficiency. The maximum daily efficiency efficiency was 16.64%, with a potential for slightly higher values in optimized designs and favorable weather conditions. Thereafter, the drying efficiency started decreasing drastically, which is mostly attributed to a lower drying rate when approaching equilibrium conditions (as evidenced by the reduced rate of moisture removal after the 6$^{\text{th}}$ day of radiant exposure) and also because of oil accumulation in the upper layer as a result of its lower density, which hinders moisture vaporization. In order to prevent the negative effects of oil accumulation on the system performance, a proposal to improve the prototype would be to include a stirring mechanism, such as a small motor connected to a propeller, which homogenizes the mixture. In addition, as the sample dries, the moisture removal capacity decreases, as the point of maximum moisture extraction is approached.

The performance of the solar still prototype was satisfactorily validated for the target application, which is the development of a passive drying system with very low energy consumption and maintenance costs, in addition to the possibility of recovering water for field irrigation. Unlike traditional rotary drum dryers, which operate continuously, the prototype solar still developed in this work operates through a discontinuous process, namely, in batches. Therefore, although both processes are not strictly comparable, it should be noted that solar dryers are clearly outperformed in terms of drying time and drying thermal efficiency by rotary drum dryers, which represent one of the most widespread options for the management of olive pomace. Modern industrial rotary drum dryers operating with olive pomace have a relatively short residence time in the range of several tens of minutes (*4*, *7*), while solar dryers require comparatively longer drying periods, usually longer than one day and up to one or two weeks. The drying thermal efficiency (η_{th}) of rotary drum dryers is often between 35–70% (*16*), whereas solar dryers exhibit comparatively lower thermal efficiencies, typically below 30% (*16*). By way of illustration, a drying thermal efficiency of 58.8% was recently predicted for the drying process of olive pomace from an initial moisture content of 65% down to a 12.5% (wet basis) in a co-current flow rotary drum dryer (*7*). The thermal requirement of such dryer was estimated at approximately 3.80 MJ/kg of evaporated water, which is markedly below the specific energy consumption of the solar still prototype developed in the present work. As another example, an experimental study on the performance of an industrial rotary drum dryer with a processing capacity of 12,500 kg/h of wet olive pomace from an from an initial moisture content of 45.2% to a final moisture content of 15% (wet basis) revealed a drying thermal efficiency of 54% and a specific energy consumption of 4.74 MJ/kg (*4*), clearly below the figures reported in Table 4 for the solar still prototype. Nevertheless, despite their better performance in terms of drying time and drying thermal efficiency, rotary drum dryers require fuel consumption (4, 7–9), usually either natural gas or exhausted olive pomace, which poses a heavy economic and environmental burden. By contrast, solar dryers are characterized by the use of a free, non-polluting, renewable, abundant energy source that cannot be monopolized (16). Moreover, as an additional advantage, the solar still prototype developed in this work allows the extraction of water for field irrigation and lacks moving parts, which reduces maintenance.

5. Discussion and conclusions

5.1. *Physical prototype*

In this work, a solar still prototype was designed and developed as a complement to the conventional drying process of olive pomace, which is currently dominated by fossil fuels. A major challenge presented by this system is that it is designed to operate in batches, not continuously as with rotary drum dryers. It presents a relatively low efficiency, when operating passively, which could be improved with the aid of an auxiliary drying system (through resistors powered by photovoltaic panels), but would have an impact on an increase in the initial investment. Finally, the increase in the cost of raw materials must be also be considered, and in particular that of materials such as stainless steel. Despite the foregoing, this system may represent a convenient improvement for olive oil producers, who bear the expenses of transportation of the wet pomace to olive pomace oil extraction plants, by reducing the weight to be transported. In addition, the solar still prototype can operate with only solar energy and very little maintenance and, unlike other management alternatives, the developed system allows obtaining water as a by-product, the reuse of which is of great importance, particularly in dry climates.

The solar still prototype was able to reduce the moisture content of the 11.28 kg sample of olive pomace from 67.17% to 39.90% without need for input of any conventional energy source, only through solar action, in a period of 10 days. Moreover, 2.4 liters of water were obtained as a by-product of the process, which represents 21.28% by weight of the sample. The amount of evaporated moisture during the 10-day period was 3.08 liters, so the efficiency of moisture recovery for irrigation was approximately 78%. Even though the solar still prototype has a relatively low efficiency, it should be highlighted that no fuel consumption is required. A major disadvantage of the developed solar still prototype is that the drying of olive pomace using the system proposed here can only be effectively used in terms of moisture recovery for irrigation applications during the cold months in autumn and winter. This is because contact with the cold glass surface favors condensation of the evaporated moisture. However, the cold months coincide with the seasonal production of olive pomace, which is ideal for the proposed application.

During the testing process, it was noted that olive oil accumulated on the upper surface, creating a thin surface layer due to stratification of the oil and water contained in the olive pomace. This remaining olive pomace oil, which can be detrimental to the drying stage, has an economic value, and thus, it is typically recovered in olive pomace extraction plants. Accordingly, any separation process that allows recovering the pomace oil is beneficial. In order to facilitate the extraction of part of this oil, the sample was placed on a platform whose contact surface is a sieve. This pattern allows the oil to permeate by separating from the olive pomace. With this simple step, it was possible to separate a large part of the remaining moisture from the olive pomace sample thanks to the action of time and the greenhouse effect that occurs inside. Accumulation of the olive pomace oil in the upper layer of the sample is detrimental to the drying process of the pomace. An improvement that could be considered to facilitate moisture removal would be the incorporation of a stirring mechanism driven by an electric motor, which would be in charge of homogenizing the sample, thereby hindering the accumulation of olive oil during the first stages of the drying process and increasing the drying performance. Alternatively, another approach to improving the drying performance is to introduce constructive improvements, such as heating the lower surface by means of heating elements powered by solar photovoltaic energy or solar thermal energy. This would allow increasing the drying rate without the need for mobile parts. An additional improvement of the prototype to recover distilled water, would be to apply a small layer of hydrophobic coating, which would facilitate the sliding of water on the glass surface. This approach would be interesting considering the losses of evaporated moisture that occur when opening the device to perform the loading and cleaning operations.

5.2. *Electronic prototype*

The developed sensor system collects and analyses the data remotely, allowing to visualize the evolution of the system and react to any complication in a simpler way, without having to physically interact with the system. To facilitate the analysis of data in real time, a graphical user interface was included. In addition, as it is an autonomous system powered by battery, which in turn is charged by a photovoltaic panel, potential issues with the power supply are eliminated. This allows a greater ease for its transfer and maintenance by not having to consider the dangers of working with high voltage. The hardware components were chosen to ensure functionality, low cost, and low energy consumption with an optimized size, providing flexibility to the system by incorporating connectors that allow adding different sensors or actuators which use the I2C protocol.

Nomenclature

Math symbols

E	Solar irradiance [W·m^{-2}]
H	Solar radiant exposure [MJ·m^{-2}]
Δh_{vap}	Specific vaporization [kJ·kg^{-1}]
m	Mass [kg]
r	Drying rate [kg moisture/day]
S_{glass}	Glass surface [m^2]
t	Time [day]
W	Moisture content, wet basis [kg moisture/kg wet sample]
X	Moisture content, dry basis [kg moisture/kg dry sample]
η_{th}	Drying thermal efficiency

Abbreviations

db	Dry basis
DMS	Degrees Minutes Seconds
HHV	Higher Heating Value [MJ·kg^{-1}]
I2C	Inter-Integrated Circuit
IoT	Internet of Things

JSON JavaScript Object Notation
LHV Lower Heating Value [MJ·kg^{-1}]
NTP Network Time Protocol
OTA Over The Air
PCB Printed Circuit Board
PSTN Public Switched Telephone Network
RH Relative Humidity
RTC Real Time Clock
RTOS Real Time Operating System
SD Secure Digital
SEC Specific Energy Consumption [MJ/kg moisture]
SMER Specific Moisture Extraction Rate [g moisture/MJ]
SoC System on Chip
SPI Serial Peripheral Interface
TCP/IP Transmission Control Protocol/Internet Protocol
UART Universal Asynchronous Receiver-Transmitter
wb Wet basis

Acknowledgements

The icons used in some figures of this article were designed by Smashicons, Freepik, Deemakdaksina, Juicy_fish and Good Ware from www.flaticon.com.

Disclosure statement

The authors report there are no competing interests to declare.

Funding

This research work was supported by the project entitled "Hacia una producción sostenible y sin residuos en la industria oleícola: un modelo de economía circular" (Ref. No. 1381442), co-funded by *Programa Operativo FEDER 2014–2020* and *Consejería de Economía y Conocimiento de la Junta de Andalucía* of the Spanish Government. R. Aguado Molina gratefully acknowledges financial support from *Ministerio de Universidades* under the FPU Program (Ref. FPU19/00930).

References

(1) Montero, I.; Miranda, M.T.; Sepúlveda, F.J.; Arranz, J.I.; Rojas, C.V.; Nogales, S. Solar Dryer Application for Olive Oil Mill Wastes, *Energies* **2015**, *8* (12), 14049–14063.
(2) Pantziaros, A.G.; Trachili, X.A.; Zentelis, A.D.; Sygouni, V.; Paraskeva, C.A. A new olive oil production scheme with almost zero wastes, *Biomass Conv. Bioref.* **2021**, *11*, 547–557.
(3) Arjona, R.; García, A.; Ollero, P. The drying of alpeorujo, a waste product of the olive oil mill industry, *J. Food Eng.* **1999**, *41* (3), 229–234.
(4) Gómez-de la Cruz, F.J.; Casanova-Peláez, P.J.; Palomar-Carnicero, J.M.; Cruz-Peragón,

F. Characterization and analysis of the drying real process in an industrial olive-oil mill waste rotary dryer: A case of study in Andalusia, *Appl. Therm. Eng.* **2017**, *116*, 1–10.
(5) Baysan, U.; Koç, M.; Güngör, A.; Ertekin, F.K. Investigation of drying conditions to valorize 2-phase olive pomace in further processing, *Dry. Technol.* **2022**, *40* (1), 65–76.
(6) Alburquerque, J.A.; Gonzálvez, J.; García, D.; Cegarra, J. Agrochemical characterisation of "alperujo", a solid by-product of the two-phase centrifugation method for olive oil extraction, *Bioresour. Technol.* **2004**, *91* (2), 195–200.
(7) Aguado, R.; Vera, D.; Jurado, F.; Beltrán, G. An integrated gasification plant for electric power generation from wet biomass: toward a sustainable production in the olive oil industry, *Biomass Conv. Bioref.* **2022**.
(8) Gómez-de la Cruz, F.J.; Palomar-Carnicero, J.M.; Hernández-Escobedo, Q.; Cruz-Peragón, F. Determination of the drying rate and effective diffusivity coefficients during convective drying of two-phase olive mill waste at rotary dryers drying conditions for their application, *Renew. Energy* **2020**, *153*, 900–910.
(9) Castaño, F.; Rubio, F.R.; Ortega, M.G. Modeling of a Cocurrent Rotary Dryer, *Dry. Technol.* **2012**, *30* (8), 839–849.
(10) Agencia Andaluza de la Energía (AAE). La bioenergía en Andalucía, https://www.agenciaandaluzadelaenergia.es/sites/default/files/Documentos/3_2_0068_20_LA_BIOENERGIA_EN_ANDALUCIA.PDF, 2020. Accessed: 2022-10-12.
(11) Montero, I.; Blanco, J.; Miranda, T.; Rojas, S.; Celma, A. Design, construction and performance testing of a solar dryer for agroindustrial by-products, *Energy Convers. Manage.* **2010**, *51* (7), 1510–1521.
(12) Ferentinos, K.P.; Katsoulas, N.; Tzounis, A.; Bartzanas, T.; Kittas, C. Wireless sensor networks for greenhouse climate and plant condition assessment, *Biosyst. Eng.* **2017**, *153*, 70–81.
(13) Benghanem, M. Measurement of meteorological data based on wireless data acquisition system monitoring, *Appl. Energy* **2009**, *86* (12), 2651–2660.
(14) Sharma, A.; Chen, C.; Vu Lan, N. Solar-energy drying systems: A review, *Renew. Sust. Energ. Rev.* **2009**, *13* (6), 1185–1210.
(15) Kumar, P.; Singh, D. Advanced technologies and performance investigations of solar dryers: A review, *Renew. Energy Focus* **2020**, *35*, 148–158.
(16) Mujumdar, A.S. *Handbook of Industrial Drying*, 4th ed.; CRC Press, 2014.
(17) Kamarulzaman, A.; Hasanuzzaman, M.; Rahim, N. Global advancement of solar drying technologies and its future prospects: A review, *Solar Energy* **2021**, *221*, 559–582.
(18) Ekechukwu, O. Review of solar-energy drying systems I: an overview of drying principles and theory, *Energy Convers. Manag.* **1999**, *40* (6), 593–613.
(19) Ekechukwu, O.V.; Norton, B. Review of solar-energy drying systems II: An overview of solar drying technology, *Energy Convers. Manag.* **1999**, *40* (6), 615–655.
(20) Ekechukwu, O.; Norton, B. Review of solar-energy drying systems III: low temperature air-heating solar collectors for crop drying applications, *Energy Convers. Manag.* **1999**, *40* (6), 657–667.
(21) Sharma, V.K.; Colangelo, A.; Spagna, G. Experimental investigation of different solar dryers suitable for fruit and vegetable drying, *Renew. Energy* **1995**, *6* (4), 413–424.
(22) Sayigh, A.A.M. Renewables: The Energy for the 21st Century, In *World Renewable Energy Congress VI*, 2000; p 634.
(23) Castillo Téllez, M.; Pilatowsky Figueroa, I.; Castillo Téllez, B.; López Vidaña, E.C.; López Ortiz, A. Solar drying of Stevia (Rebaudiana Bertoni) leaves using direct and indirect technologies, *Solar Energy* **2018**, *159*, 898–907.
(24) Vijayavenkataraman, S.; Iniyan, S.; Goic, R. A review of solar drying technologies, *Renew. Sust. Energ. Rev.* **2012**, *16* (5), 2652–2670.
(25) Moheno-Barrueta, M.; Tzuc, O.M.; Martínez-Pereyra, G.; Cardoso-Fernández, V.; Rojas-Blanco, L.; Ramírez-Morales, E.; Pérez-Hernández, G.; Bassam, A. Experimental Evaluation and Theoretical Optimization of an Indirect Solar Dryer with Forced Ventilation under Tropical Climate by an Inverse Artificial Neural Network, *Appl. Sci.* **2021**, *11* (16).

(26) Sharma, V.K.; Colangelo, A.; Spagna, G. Experimental performance of an indirect type solar fruit and vegetable dryer, *Energy Convers. Manag.* **1993**, *34* (4), 293–308.
(27) ben Mabrouk, S.; Belghith, A. Development of the solar crop dryers in Tunisia, In *World Renewable Energy Congress VI*, 2000; pp 2206–2211.
(28) Fudholi, A.; Sopian, K.; Alghoul, M.; Ruslan, M.H.; Othman, M.Y. Performances and improvement potential of solar drying system for palm oil fronds, *Renew. Energy* **2015**, *78*, 561–565.
(29) Shamekhi-Amiri, S.; Gorji, T.B.; Gorji-Bandpy, M.; Jahanshahi, M. Drying behaviour of lemon balm leaves in an indirect double-pass packed bed forced convection solar dryer system, *Case Stud. Therm. Eng.* **2018**, *12*, 677–686.
(30) Nindo, C.I.; Kudo, Y.; Bekki, E. Test Model for Studying Sun Drying of Rough Rice Using Far-Infrared Radiation, *Dry. Technol.* **1995**, *13* (1-2), 225–238.
(31) Zomorodian, A.A.; Dadashzadeh, M. Indirect and Mixed Mode Solar Drying Mathematical Models for Sultana Grape, *J. Agr. Sci. Tech.* **2009**, *11* (4), 391–400.
(32) Baniasadi, E.; Ranjbar, S.; Boostanipour, O. Experimental investigation of the performance of a mixed-mode solar dryer with thermal energy storage, *Renew. Energy* **2017**, *112*, 143–150.
(33) Yassen, T.A.; Al-Kayiem, H.H. Experimental investigation and evaluation of hybrid solar/thermal dryer combined with supplementary recovery dryer, *Solar Energy* **2016**, *134*, 284–293.
(34) Perea-Moreno, A.J.; Juaidi, A.; Manzano-Agugliaro, F. Solar greenhouse dryer system for wood chips improvement as biofuel, *J. Clean. Prod.* **2016**, *135*, 1233–1241.
(35) Shimpy; Kumar, M.; Kumar, A. Performance Assessment and Modeling Techniques for Domestic Solar Dryers, *Food Eng. Rev.* **2020**.
(36) National Aeronautics and Space Administration (NASA). POWER Data Access Viewer, https://power.larc.nasa.gov/data-access-viewer. Accessed: 2022-10-12.
(37) Agencia Andaluza de la Energía (AAE). Radiación solar, https://www.agenciaandaluzadelaenergia.es/Radiacion/radiacion1.php. Accessed: 2022-10-12.
(38) Chavan, A.; Thorat, B. Techno-economic comparison of selected solar dryers: A case study, *Dry. Technol.* **2022**, *40* (10), 2105–2115.